A boundary-layer model of thermocapillary flow in a cold corner

D. Canright
Mathematics Department, Code MA/Ca, Naval Postgraduate School, Monterey, California 93943

M. Huber
Mathematical Sciences Department, U.S. Military Academy, West Point, New York 10996

(Received 12 October 2001; accepted 6 June 2002)

This work develops a boundary-layer model for the thermocapillary feedback mechanism that can occur at the edge of weld pools and other materials processes, in the limit where convection dominates the heat transport but the Prandtl number is small. Previously, Canright [Phys. Fluids **6**, 1415 (1994)] showed that in this regime the dynamics of this ''cold corner'' region is locally determined through the thermal gradient driving the convection that contains the gradient. The present work applies standard boundary-layer approximations to construct a model that captures this dominant feedback mechanism and agrees well with a purely numerical model. © *2002 American Institute of Physics.* [DOI: 10.1063/1.1498117]

I. INTRODUCTION

Many materials processes involve a pool of molten material with a free surface. In some cases thermocapillary forces predominate in driving vigorous convection in the melt, at least in certain regions (i.e., cold corner regions[1]) or in low gravity. Reviews of some relevant studies of thermocapillary flows, both numerical and analytical, are given by Ostrach[2] and by Davis.[3] Some careful numerical studies, e.g., those of Zebib *et al.*[4] and Zehr *et al.*,[5] have shown strong thermocapillary convection and heat transfer in a small region where the liquid meets the relatively cool solid, at least for small Prandtl number. The small length scales in this ''cold corner'' region result from a sort of positive feedback, where the surface thermal gradient drives the convection that compresses the thermal gradient. Great care is necessary to resolve the small length scales of this region numerically.

In previous work, Canright[6] explored the scaling of the cold corner region in two dimensions, analytically and numerically, and showed that for sufficiently strong convection, i.e., high Marangoni number, the corner dynamics and scaling are *locally* determined, relatively unaffected by conditions far from the corner. For such cases where additionally the Prandtl number is small, and hence the Reynolds number is high, thin viscous boundary layers form within the corner region, preventing the vorticity from diffusing into the main flow. The present work develops a boundary layer model for this case.

Standard boundary layer techniques are applied to give approximate descriptions of the viscous boundary layers along the free surface and the solid boundary. The entrainment into the boundary layers drives the irrotational flow in the ''core'' region, outside the boundary layers. The core flow is used in numerically solving the convection-diffusion heat equation. The resulting surface thermal gradient is used to update the surface boundary layer. This cycle is iterated to convergence, giving a consistent approximate description of the cold corner feedback region. This model, with no adjustable parameters, agrees well with the purely numerical results.[6]

This model of the rapid convection and high heat transfer in the cold corner may be useful as a local description, when coupled to numerical investigations of the overall behavior of the melt in materials processes. Such use would obviate the otherwise severe numerical requirements of resolving the small length scales of this important region of high heat transfer.

This work is organized as follows. We define the problem in Sec. II and also correct the scaling of Canright.[6] In Sec. III we exploit the boundary-layer structure to derive the leading-order equations for each region. Section IV gives analytic solutions for the flow inside and outside the boundary layers, and describes the numerical solution method for the thermal field. Results and conclusions comprise the last two sections.

II. PROBLEM STATEMENT AND SCALING

The present work analyzes a particular parameter regime of the problem examined by Canright.[6] (The analysis below was shown in much greater detail by Huber.[7]) A pool of incompressible Newtonian fluid is bounded on the left by a vertical solid wall, piecewise isothermal, cold to depth d and hot below, while the fluid far from the corner is at the hot ambient temperature: See Fig. 1. Above the horizontal free surface of the liquid is an inviscid, nonconducting gas. Surface tension is assumed strong enough to keep the free surface flat (small Capillary number), but with surface tension variations due to a linear dependence on temperature. Gravity is neglected. The resulting flow is assumed to be two-dimensional and steady.

The corresponding dimensionless problem follows, based on the overall length scale d (from the wall boundary condition), the temperature difference ΔT, and the velocity scale $u_s \equiv \gamma \Delta T/\mu$, where γ, assumed constant and positive,

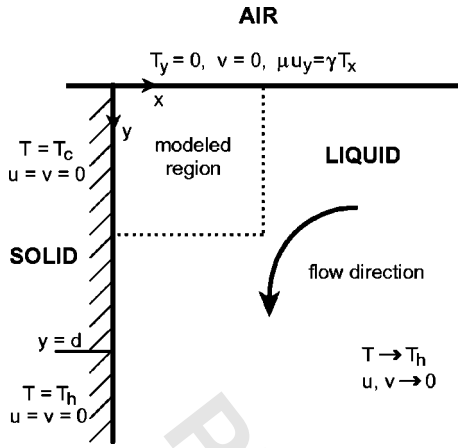

FIG. 1. Problem formulation: A liquid quarter-space is bounded above by a flat free surface subject to thermocapillary forcing, and is bounded on the left by a rigid vertical wall, at temperature T_c to depth d and at the warmer temperature T_h below, which is also the ambient temperature of the undisturbed fluid far away. The region near the corner is modeled here.

is the negative of the derivative of the surface tension with respect to temperature and μ is viscosity

$$M\mathbf{u}\cdot\nabla T=\nabla^2 T, \tag{1}$$

$$M/P\,\mathbf{u}\cdot\nabla\mathbf{u}=-\nabla p+\nabla^2\mathbf{u}, \tag{2}$$

$$\nabla\cdot\mathbf{u}=0, \tag{3}$$

with the boundary conditions

$$\text{at}\quad y=0:\quad T_y=0,\quad v=0,\quad u_y=T_x, \tag{4}$$

$$\text{at}\quad x=0:\quad T=\begin{cases}-1, & y<1\\ 0, & y>1\end{cases},\quad u=v=0, \tag{5}$$

$$\text{as}\quad x,y\to\infty:\quad T\to 0,\quad u,v\to 0. \tag{6}$$

Here $\mathbf{u}$ is the velocity vector with components u and v in the x (rightward) and y (downward) directions, p is pressure, and T is temperature. The two dimensionless parameters are the Marangoni number $M\equiv u_s d/\kappa$ and the Prandtl number $P\equiv\upsilon/\kappa$, where κ is the thermal diffusivity and υ is the kinematic viscosity. The Reynolds number is $R\equiv M/P$.

With two independent parameters there are four different asymptotic regimes of behavior. The regime we consider here is where the flow is strong enough to compress the thermal gradient against the wall and the viscosity is small enough that vorticity is confined to thin boundary layers along the surface and the wall, around an essentially irrotational core region. These viscous boundary layers are within the compressed thermal region, as seen in the prior numerical results;[6] this is the region we analyze here.

Following Canright,[6] let the velocity scale along the surface be U, the horizontal length scale of the temperature variation be l, and the vertical thickness of the surface viscous boundary layer be δ. From the thermocapillary condition (4c), $U/\delta\sim 1/l$. Then by continuity (3), where the boundary layer meets the core, $\upsilon\sim(\delta/l)U\sim(\delta/l)^2$.

If the horizontal velocity in the core is of the same scale as that along the surface, as assumed in previous work,[6] then the vorticity in the core scales as $\omega\equiv v_x-u_y\sim(U\delta/l^2)-(U/l)\sim U/l$, which is of the same order as the velocity gradient. This is inconsistent with the core flow being essentially irrotational, with vorticity confined to the boundary layers, as is seen in the numerical results. Hence the core velocity scale in both directions must be that of υ, i.e., $(\delta/l)^2$.

In the surface boundary layer, convection and vertical diffusion of momentum are both important, so from (2), $(M/P)U^2/l\sim U/\delta^2$. In the core, outside the viscous boundary layers, convection of heat balances diffusion, so (1) gives $M(\delta/l)U(1/l)\sim 1/l^2$. Solving gives these scales: $l\sim M^{-1}P^{-2}$, $\delta\sim M^{-1}P^{-1}$, $U\sim P$, with the core velocity scale P^2. This regime applies as long as diffusion of momentum is negligible in the core and the horizontal thermal length scale is much smaller than the vertical, giving $M\gg P^{-2}$, $P\ll 1$.

This correction modifies the scaling analysis in Canright[6] in the convective inertial regime. Similar reasoning applies in the conductive inertial regime. This gives the scalings $l\sim 1$, $U\sim\delta\sim(P/M)^{1/3}$, as previously,[6] but with the core velocity scale $(P/M)^{2/3}$. The range of the conductive inertial regime is changed to $P\ll M\ll P^{-2}$, $P\ll 1$. Note that all these corrected scalings retain the same dependence on the Marangoni number as given by Canright;[6] only the Prandtl number dependence has changed.

III. BOUNDARY LAYER STRUCTURE

For small Prandtl number and sufficiently large Marangoni number (the convective inertial regime) the vigorous cold-corner convection is limited to a region of size $l\ll 1$, and within this region relatively thin ($\delta\ll l$) viscous boundary layers occur along the thermocapillary-driven surface and along the rigid wall. The dynamics of this region are *locally* determined[6] and the local *effective* Marangoni number is unity; hence M does not appear in the appropriately rescaled equations. Here we apply boundary layer techniques to model how these thin viscous layers interact with thermal convection in the core region, outside the viscous layers.

For this regime, locally rescaling the problem using the core scales (lengths $\sim M^{-1}P^{-2}$ and velocities $\sim P^2$) gives the system below

$$UT_X+VT_Y=T_{XX}+T_{YY}, \tag{7}$$

$$UU_X+VU_Y=-p_X+P(U_{XX}+U_{YY}), \tag{8}$$

$$UV_X+VV_Y=-p_Y+P(V_{XX}+V_{YY}), \tag{9}$$

$$U_X+V_Y=0, \tag{10}$$

where subscripts indicate partial derivatives, with the boundary conditions

$$\text{surface}\quad Y=0:T_Y=0, \tag{11}$$

$$V=0, \tag{12}$$

$$P^2U_Y=T_X, \tag{13}$$

$$\text{wall}\quad X=0:T=-1, \tag{14}$$

$$U=0, \tag{15}$$

$$V=0, \tag{16}$$

$$\text{far away } X,Y\to\infty: T\to 0, \tag{17}$$

$$U\to 0, \tag{18}$$

$$V\to 0. \tag{19}$$

Here uppercase letters are used for the variables scaled in this way: U, V, X, and Y. Pressure is still lowercase p. Note that the wall is isothermal on this scale.

Following standard boundary-layer methods, we break up the problem into separate regions: The core region, a horizontal boundary layer along the surface, and a vertical boundary layer along the wall. Relative to the core region, the boundary layers are thin, by a factor of P, with the component of velocity along the boundary being large, by a factor of P^{-1}. We will use lowercase letters to indicate variables scaled appropriately for the boundary layers, e.g., in the surface layer $y=Y/P$ and $u=PU$. We decompose the problem into separate regions below, including only terms of leading-order as $P\to 0$.

A. Surface boundary layer

Applying the standard boundary layer approximation gives the following system for the flow in the surface layer:

$$uu_X+Vu_y=u_{yy}, \tag{20}$$

$$u_X+V_y=0, \tag{21}$$

with the boundary conditions

$$\text{surface } y=0: u_y=T_X, \tag{22}$$

$$V=0, \tag{23}$$

$$\text{match to core } y\to\infty: u\to 0, \tag{24}$$

$$\text{upstream } X\to\infty: u\to 0. \tag{25}$$

Note that, because the core flow is of a higher order (size P smaller), the pressure term of the standard boundary layer equation does not appear, and the matching condition to the core flow is homogeneous. Thus, to leading order, the surface flow is *entirely* determined by the surface thermal gradient.

This leads to a net mass flux towards the wall, as $x\to 0$. Since the wall is impermeable, the boundary layer approximation must break down in some small sub-region, whose size is of the same order as the boundary layer thickness, where the flow turns the corner to flow down the wall. This gives the initial condition for the flow in the wall boundary layer; the actual matching condition used will be discussed later, along with the solution methods.

B. Wall boundary layer

Similarly, the standard approach describes the flow down the wall, starting from an initial net flux (like a wall jet), by the system

$$Uv_x+vv_Y=v_{xx}, \tag{26}$$

$$U_x+v_Y=0, \tag{27}$$

with the boundary conditions

$$\text{wall } x=0: U=0, \tag{28}$$

$$v=0, \tag{29}$$

$$\text{match to core } x\to\infty: v\to 0, \tag{30}$$

where the initial condition at $Y\to 0$, matching to the flux from the surface layer, will be defined below. Again, the core flow is negligible, so the wall layer depends only on the initial condition.

C. Core flow

To leading order, the core flow is irrotational, since the viscous terms are of order P and the flow upstream goes to zero. (This assumption seems to agree reasonably well with previous numerical results, where the vorticity generated by the surface and wall appears to be confined primarily to the boundary layers.) Then the core potential flow is determined by the normal component of velocity on the boundaries, i.e., by entrainment into the boundary layers. The stream function ψ satisfies Laplace's equation

$$\psi_{XX}+\psi_{YY}=0, \tag{31}$$

$$U=\psi_Y, \quad V=-\psi_X, \tag{32}$$

with the asymptotic matching conditions

$$\text{surface: } \lim_{Y\to 0} V_{\text{core}}(X,Y)=\lim_{y\to\infty} V_{\text{surface}}(X,y), \tag{33}$$

$$\text{wall: } \lim_{X\to 0} U_{\text{core}}(X,Y)=\lim_{x\to\infty} U_{\text{wall}}(x,Y), \tag{34}$$

$$\text{far away } X,Y\to\infty: U,V\to 0. \tag{35}$$

D. Core thermal field and matching

The heat balance in the core is governed by the convection-diffusion equation (7), where the velocity field is the core potential flow.

Because the boundary layers are thin relative to the core thermal variations, they might be expected to play no role in the thermal boundary conditions. However, flow in the boundary layers is fast, so thermal convection in the layers can affect the heat balance. To examine this effect in the surface layer, assume the core temperature field $T(X,Y)$ has an additional small perturbation $Pt(X,y)$ in the layer, due to the fast flow $P^{-1}u(X,y)$ there. Then the heat equation (7) becomes, in the surface layer:

$$P^{-1}u(T_X+Pt_X)+V(T_Y+t_y)$$
$$=(T_{XX}+Pt_{XX})+(T_{YY}+P^{-1}t_{yy}), \tag{36}$$

or, to leading order

$$uT_X=t_{yy}, \tag{37}$$

where T_X is independent of y through the layer, and the insulated surface boundary condition (11) becomes

$$T_Y(X,0)+t_y(X,0)=0. \tag{38}$$

Outside the layer, the fast flow and thus the thermal perturbation disappear:

$$\text{as } y\to\infty: t\to 0 \quad (\text{and } u\to 0). \tag{39}$$

Integrating (37) with the above conditions gives the surface matching condition for the core temperature

$$\text{surface: } T_Y(X,0)=T_X(X,0)\int_0^\infty u(X,y)dy. \tag{40}$$

The thermal convection in the layer acts as a heat source to the core.

Applying a similar approach to the wall layer shows that, because the wall is isothermal, there is no leading-order thermal effect of the fast flow down the thin wall layer. So the remaining conditions on the core heat are as before (14) and (17).

IV. SOLUTION

Based on this boundary layer structure, our overall solution scheme is iterative:

(1) Assume some initial surface thermal gradient $T_X(X,0)$;
(2) solve the surface flow driven by the thermal gradient;
(3) solve the wall flow from the surface flow turning the corner;
(4) solve the core flow from entrainment into the boundary layers;
(5) find the resulting temperature field in the core $T(X,Y)$;
(6) if the solution has not yet converged, go back to step 2.

The methods we used for each step are detailed below.

A. Surface boundary layer

In typical laminar boundary layers by solid surfaces, the no-slip condition generates vorticity at the surface, which is convected along the surface due to the external flow. We adapted the method of Timman,[8] developed for the usual case, to the surface layer in our problems (20)–(25), where the thermocapillary stress generates vorticity and also induces the flow along the surface, while the external flow is negligible.

Timman[8] assumed a velocity profile of the form

$$\frac{u}{U}=f(\eta)=1-\int_\eta^\infty e^{-\eta^2}(a+c\eta^2+\cdots)d\eta - e^{-\eta^2}(b+d\eta^2+\cdots), \tag{41}$$

where $\eta=y/\delta(X)$, with $\delta(X)$ indicating the layer thickness, and the coefficients a, b, c, and d, etc., are functions of X.

For our purposes, a single-term profile suffices with the velocity decaying to zero:

$$u=f(\eta)=\int_\eta^\infty a(X)e^{-t^2}dt=\frac{a(X)\sqrt{\pi}}{2}\operatorname{erfc}(\eta). \tag{42}$$

Then the surface shear stress is

$$u_y(X,0)=\frac{f'(0)}{\delta(X)}=\frac{-a(X)}{\delta(X)}=T_X, \tag{43}$$

where the last equality is due to the thermocapillary condition (22).

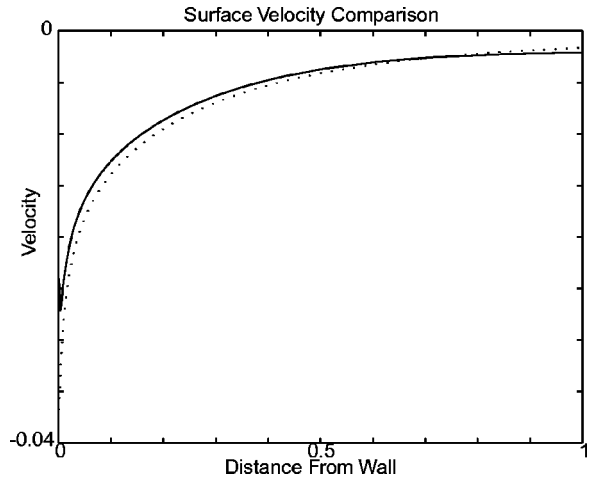

FIG. 2. Comparison of surface velocity profiles from numerical data of Canright (Ref. 6) (solid) and Timman's method prediction (dotted) based on the numerical temperature gradient. (The numerical data for all comparisons used $M=10\,000$ and $P=0.01$.h.)

Following Timman, we define the momentum thickness δ_2 as

$$\delta_2\equiv\int_0^\infty u^2dy=\frac{a^2(X)\pi}{4}\delta(X)\int_0^\infty[\operatorname{erfc}(\eta)]^2d\eta, \tag{44}$$

and the surface stress can be written in terms of the momentum thickness as

$$u_y(X,0)=-\frac{d}{dX}(\delta_2)=T_X. \tag{45}$$

Since far upstream both the thermal gradient and the velocity vanish, solving yields

$$\delta_2=-T. \tag{46}$$

Thus we can solve for the boundary layer thickness, giving

$$\delta(X)=\left[-\frac{T}{T_X^2\varepsilon}\right]^{1/3}. \tag{47}$$

where

$$\varepsilon=\frac{\pi}{4}\int_0^\infty[\operatorname{erfc}(\eta)]^2d\eta=\frac{\sqrt{\pi}}{2}\left(1-\frac{\sqrt{2}}{2}\right). \tag{48}$$

Then the resulting velocity model is

$$u=-\frac{\sqrt{\pi}}{2}\varepsilon^{-1/3}(-T)^{1/3}(T_X)^{1/3}\operatorname{erfc}(\eta). \tag{49}$$

and the stream function indicates the mass flux in the layer:

$$\psi_{\text{surface}}(X,y)=\int u\,dy=-\left[\frac{(-T)^2}{\varepsilon^2T_X}\right]^{1/3}\times\left[\frac{1-e^{-\eta^2}}{2}+\frac{\sqrt{\pi}}{2}\eta\operatorname{erfc}(\eta)\right]. \tag{50}$$

For comparison, we used previous numerical surface temperature data[6] to calculate the surface velocity from (49). Figure 2 shows this boundary-layer velocity (dotted) along

with the numerical velocity data from Canright[6] (solid). The excellent agreement validates this simple model of the thermocapillary layer. Taking a vertical profile of u through the boundary layer also gives reasonably good agreement between the predicted shape and the numerical data.

Note: the numerical data for this and all later comparisons was calculated with the parameters $M=10\,000$, $P=0.01$. But since this cold corner region is locally determined, independent of the global length scale, then the *local, effective* Marangoni number is $M_{\text{eff}}=1$, giving a local, effective Reynolds number $R_{\text{eff}}=100$. These numerical results do exhibit the local structure assumed here.

B. Wall boundary layer

We assume that the rapid flow along the free surface towards the wall turns to flow down the wall, in some small subregion near the origin where the boundary layer approximations do not apply. Then this initially concentrated flow down the wall into passive fluid forms a plane wall jet, governed by (26)–(30).

The wall jet is not constrained by any external length scale, so an appropriate model is the similarity solution of Glauert[9]

$$\psi_{\text{wall}}(x,Y)=-(40FY)^{1/4}f(\eta), \tag{51}$$

$$\eta=\left(\frac{5F}{32Y^3}\right)^{1/4}x, \tag{52}$$

where the profile $f(\eta)$ is given implicitly by

$$\eta=\ln\left(\frac{\sqrt{g^2+g+1}}{(1-g)}\right)+\sqrt{3}\arctan\left(\frac{\sqrt{3}g}{2+g}\right). \tag{53}$$

with $f=g^2$, and the scaling factor F is defined as

$$F=\int_0^\infty v\left(\int_x^\infty v^2dx'\right)dx, \tag{54}$$

which is constant along the wall jet. Then the velocity may be written as

$$v=\left(\frac{5F}{2Y}\right)^{1/2}f'(\eta). \tag{55}$$

The shape of this velocity profile (55) resembles typical velocity profiles near the wall from the prior numerical data.[6]

This similarity solution for the wall jet depends only on the quantity F, which Glauert terms the ''flux of the external momentum flux.'' For our problem, we need to find a way to match the surface layer flow toward the wall to the strength of the wall jet down the wall. Note, however, that the similarity solution is singular at the origin $Y=0$, where the peak velocity becomes infinite while the mass flux goes to zero, so applying matching at the origin is impossible.

Glauert suggests one way to estimate the magnitude of F, by

$$F\approx\tfrac{1}{2}(\text{typical velocity})\times(\text{mass flux})^2. \tag{56}$$

But if we use the typical velocity and mass flux from the surface layer [from (49) and (50)] we get $F\propto T_X^{-1/3}$, i.e., as the thermal gradient steepens and surface convection gets stronger, the wall flow gets weaker, which is not reasonable.

Instead, we match the peak surface velocity into the corner to the peak velocity in the wall layer coming out of the corner, at a distance of one boundary layer thickness down the wall to avoid the singularity

$$u_{\max}=\frac{\sqrt{\pi}}{2}\left(\frac{T_X}{\varepsilon}\right)^{1/3}=v_{\max}$$

$$=2^{-5/3}\left(\frac{c}{Y}\right)^{1/2}\quad\text{at}\quad Y=\Delta=2\left(\frac{Y^3}{c}\right)^{1/4}, \tag{57}$$

where $c=(5F/2)$ and T_X is the gradient at the origin. Solving gives

$$F=\frac{16\sqrt{\pi}}{5}\left(\frac{T_X}{2\varepsilon}\right)^{1/3}. \tag{58}$$

This matching condition for F captures the positive feedback mechanism of the cold corner, where a steeper thermal gradient gives stronger flow.

C. Core potential flow

The potential flow in the core region due to entrainment into the boundary layers (31)–(35) is expressed as the superposition of two contributions to the stream function ψ_{core}, one due to the surface layer and one due to the wall layer

$$\psi_{\text{core}}(X,Y)=\psi_{\text{core,sfc}}(X,Y)+\psi_{\text{core,wall}}(X,Y). \tag{59}$$

The first part $\psi_{\text{core,sfc}}$ is found by boundary integrals, using the Green's function for Laplace's Equation in a quarter-plane $(X>0,Y>0)$ with Dirichlet conditions

$$G(\boldsymbol{X},\boldsymbol{X}_0)=\frac{1}{4\pi}\ln\left\{\frac{[(X-X_0)^2+(Y-Y_0)^2][(X+X_0)^2+(Y+Y_0)^2]}{[(X-X_0)^2+(Y+Y_0)^2][(X+X_0)^2+(Y-Y_0)^2]}\right\}, \tag{60}$$

The boundary condition must match the stream function at the edge of the surface layer

$$\psi_{\text{core,sfc}}(X,0)=\psi_{\text{surface}}(X,\infty)$$

$$=-\tfrac{1}{2}\varepsilon^{-2/3}(-T)^{2/3}(T_X)^{-1/3}. \tag{61}$$

Then throughout the core

$$\psi(X,Y)_{\text{core,sfc}}=-\int_0^\infty\psi_{\text{surface}}(X,\infty)\left.\frac{\partial G}{\partial Y}\right|_{Y=0}dX. \tag{62}$$

Due to the singularity of the self-similar wall jet at the

origin, the zero mass flux out of the corner cannot match the mass flux into the corner from the surface layer. This would give a discontinuity in the stream function at the origin, acting as a mass source of fluid flowing radially away from the origin, which is unreasonable. To eliminate this discontinuity, the wall boundary condition on $\psi_{\text{core,sfc}}$ is modified from zero to a constant equal to the flux into the corner, $\psi_{\text{surface}}(0,\infty)$. Equivalently, a term of the form

$$\psi_{\text{correction}}(X,Y)=\psi_{\text{surface}}(0,\infty)\,\frac{2}{\pi}\arctan(Y/X), \tag{63}$$

is added to the $\psi_{\text{core,sfc}}$ from the boundary integral (62) above. Note that this correction does not affect the normal velocity matching conditions from the core to the boundary layers.

The potential flow due to the self-similar wall jet is based on the approach of Plotkin,[10] who used complex variables to find the outer potential flow induced by Glauert's solution in a half-plane. Here, we apply the boundary conditions in the quarter-plane, namely, that $\psi_{\text{core,wall}}(0,Y)=-\int_0^\infty v(x,Y)dx=-(40FY)^{1/4}$ and $\psi_{\text{core,wall}}(X,0)=0$ for $X>0$. Then the core flow from the jet flowing down the wall becomes

$$\psi_{\text{core,wall}}(X,Y)=-(40F)^{1/4}[\text{Re}((Y+iX)^{1/4}) -(1+\sqrt{2})\text{Im}((Y+iX)^{1/4})]. \tag{64}$$

D. Core thermal field

The heat in the core is governed by the convection-diffusion equation (7), with Dirichlet conditions at the wall (14), homogeneous Dirichlet conditions far away (17), and Neumann matching conditions for the heat flux from the surface boundary layer (40). But for numerical purposes, rather than solve (7) directly, instead we solve the unsteady heat equation

$$T_t+UT_X+VT_Y=T_{XX}+T_{YY}, \tag{65}$$

where t is time, until steady state is reached.

Also, artificial boundaries were introduced to modify the quarter-plane problem into a rectangle problem. The domain size and new boundary conditions were chosen to approximate the far field. Specifically, on the right boundary, $T=0$ for the hot incoming fluid, and on the bottom boundary, $T_Y=0$ to minimize downstream influence.

The alternating direction implicit (ADI) method was used to solve the two-dimensional unsteady heat equation on a uniform grid. The initial temperature field was exponentially decaying on the surface and zero elsewhere. The iterative solution involved two loops: The outer loop updated the velocity field, based on the temperature along the surface; the inner loop (a fixed number of iterations) was simply the ADI algorithm marching in time with the velocity field unchanging. Once the difference between successive temperature solutions fell below a certain tolerance, steady-state was assumed.

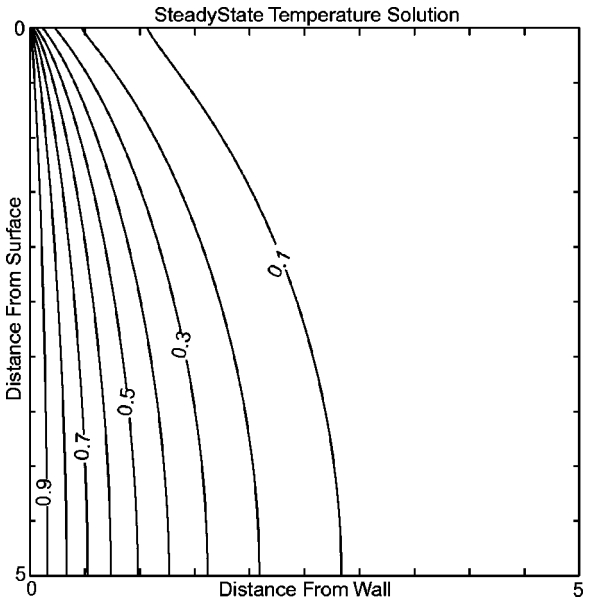

FIG. 3. Steady-state temperature: Isotherms from the ADI method, over the whole computational domain.

V. RESULTS

Figure 3 shows the steady-state temperature solution. The spatial step size is 0.01 in both directions. The thermal field is compressed against the wall by the flow into the corner. A closer view of the corner is shown in Fig. 4, which also compares our current approach (on the left) with numerical data from Canright[6] (on the right). In comparing, note that our model here is a local one, and so does not apply at the temperature discontinuity in the numerical data, where the wall boundary condition for $y>1$ was $T=0$. The comparison is encouraging, particularly since the model has no adjustable parameters.

As another comparison, surface temperatures are plotted, in Fig. 5. There is excellent agreement of the temperature gradient in the corner, where the thermocapillary feedback is strongest. The details differ farther out, but the numerical data is for somewhat different far-field conditions, including recirculating flow.

Uniform solution

To illustrate how the pieces fit together, we construct a uniformly valid composite solution for a particular value of

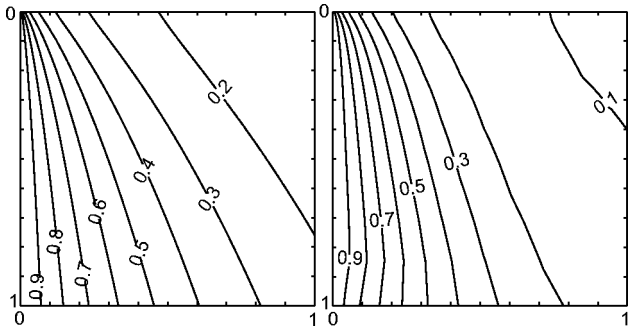

FIG. 4. Steady-state temperature detail: Isotherms of local model (left) compared to numerical data (right) from Canright (Ref. 6), over a region of size l.

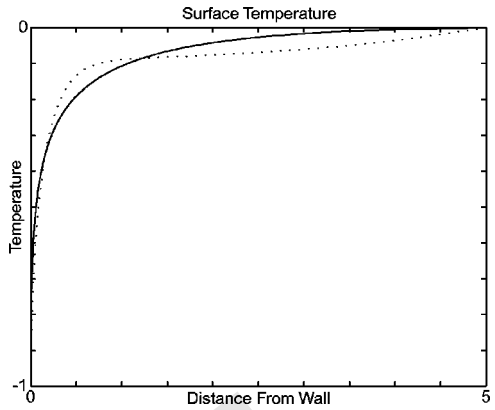

FIG. 5. Steady-state surface temperature: Current model (solid) compared to prior numerical data (Ref. 6) (dotted).

the asymptotic parameter, $P=0.01$, in the standard way. For example, the uniform stream function for the entire domain can be written as

$$\psi_{\text{uniform}}=\psi_{\text{inner}}+\psi_{\text{outer}}-\psi_{\text{match}}, \tag{66}$$

where the inner solution is composed of the flow field in the surface and wall boundary layers,

$$\psi_{\text{inner}}(X,Y)=\psi_{\text{surface}}(X,Y/P)+\psi_{\text{wall}}(X/P,Y), \tag{67}$$

the outer solution is made up of the two components of the core velocity, due to the similarity solution and the Green's function

$$\psi_{\text{outer}}(X,Y)=\psi_{\text{core,sfc}}(X,Y)+\psi_{\text{core,wall}}(X,Y), \tag{68}$$

where $\psi_{\text{core,sfc}}$ includes the correction from (63), and the matching part, representing the overlap of inner and outer solutions, comes from the matching conditions

$$\psi_{\text{match}}(X,Y)=\psi_{\text{core,sfc}}(X,0)+\psi_{\text{core,wall}}(0,Y). \tag{69}$$

This uniform stream function is shown in Fig. 6. The horizontal velocity component increases as the distance to the wall decreases, and the vertical wall jet can clearly be seen. (The wall jet flow turns out to be the strongest component of the uniform solution.)

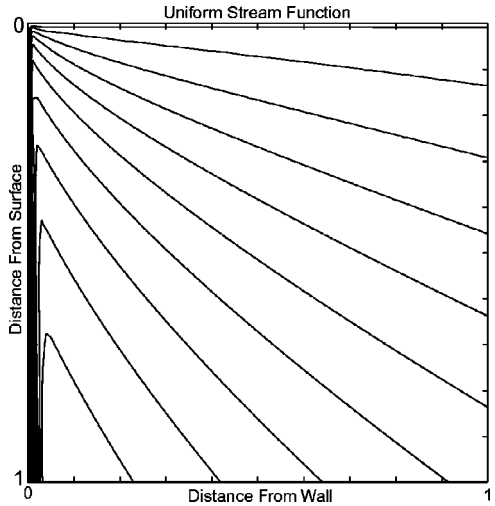

FIG. 6. Uniform stream function (detail): Streamlines of the uniform composite solution, for $P=0.01$. The strong wall jet appears clearly.

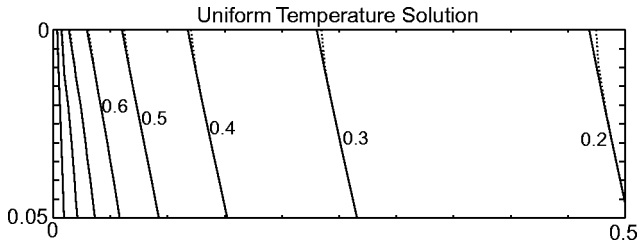

FIG. 7. Uniform temperature solution detail: Isotherms with (dotted) and without (solid) the surface convection term, for $P=0.01$ (vertical scale exaggerated).

The uniform composite form for the temperature is simply that used to find the surface heating (37), i.e.,

$$T_{\text{uniform}}(X,Y)=T_{\text{outer}}(X,Y)+P\ t_{\text{inner}}(X,Y/P). \tag{70}$$

Here $P\ t_{\text{inner}}(X,Y/P)$ is the temperature adjustment within the surface boundary layer, from (37), which decays to zero outside the surface layer, so there is no T_{match} to subtract. The T_{outer} is the temperature solution obtained from the ADI method.

As can be seen in Fig. 7, the uniform temperature solution (dotted) differs from the steady-state outer (ADI) solution (solid) only close to the surface, and only by a small amount. The uniform temperature prediction *bends* toward the surface to intersect it perpendicularly, satisfying the $T_y=0$ boundary condition.

VI. CONCLUSIONS

The results show that this boundary layer model effectively captures the dynamics of the cold corner region, in the convective inertial regime. The thermocapillary stress from the surface thermal gradient drives rapid flow in a thin layer along the surface, modeled well by a simple one-term flow profile. This surface flow depends *only* on the surface thermal gradient. In some small subregion not modeled here, the inward surface flow turns downward along the wall. This downward flow is modeled as a self-similar wall jet, where the peak velocity at a position one boundary layer thickness down is matched to the peak velocity in the surface flow. (The singularity of the similarity solution at the origin precludes matching there.) Entrainment into the boundary layers drives a weaker core flow, modeled as irrotational, combining a boundary integral term for the surface with an analytic form for the wall jet. This core flow convects heat toward the wall (solved numerically), containing the thermal gradient, and thus completing the feedback loop.

This leading-order boundary-layer model depends on a single small parameter, the Prandtl number P. That parameter only affects how thin the boundary layers are; the core flow and thermal fields do not change with P. How this local model should be *scaled* to fit the original problems (1)–(6) depends on the Marangoni number M also, of course. Hence this model could be incorporated as a local representation of the cold corner, in the context of a global numerical model

for, e.g., a weld pool. This would eliminate the need to numerically resolve the thin boundary layers, a significant computational simplification.

In future work, we hope to examine more carefully how the surface layer ''turns the corner,'' with the goal of a better matching condition with the wall layer. This would probably entail some model of the two-dimensional (2D) turning flow in the small corner subregion. Another improvement would be to consider the next terms beyond leading order, in a power series in P.

[1]M. M. Chen, ''Thermocapillary convection in materials processing,'' in *Interdisciplinary Issues in Materials Processing and Manufacturing*, ASME, edited by S. K. Samanta *et al.* (American Society of Mechanical Engineering, New York, 1987), pp. 541–557.
[2]S. Ostrach, ''Low gravity fluid flows,'' Annu. Rev. Fluid Mech. **14**, 313 (1982).
[3]S. H. Davis, ''Thermocapillary instabilities,'' Annu. Rev. Fluid Mech. **19**, 403 (1987).
[4]A. Zebib, G. M. Homsy, and E. Meiburg, ''High Marangoni number convection in a square cavity,'' Phys. Fluids **28**, 3467 (1985).
[5]R. Zehr, M. M. Chen, and J. Mazumder, ''Thermocapillary convection of a differentially heated cavity at high Marangoni numbers,'' in *ASME National Heat Transfer Conference, Pittsburgh, PA* (American Society of Mechanical Engineering, New York, 1987), paper No. 87-HT-229.
[6]D. Canright, ''Thermocapillary flow near a cold wall,'' Phys. Fluids **6**, 1415 (1994).
[7]M. R. Huber, ''A boundary layer model of thermocapillary flow in a cold corner,'' Ph.D. thesis, Naval Postgraduate School, 2000.
[8]R. Timman, ''A one-parameter method for the calculation of laminar boundary layers,'' Rep. Trans. nat. LuchtvLab., Amsterdam **15**, F29 (1949).
[9]M. B. Glauert, ''The wall jet,'' J. Fluid Mech. **1**, 625 (1956).
[10]A. Plotkin, ''A second-order correction to the Glauert wall jet solution,'' AIAA J. **8**, 189 (1970).